ARCHIVES OF ELECTRICAL ENGINEERING VOL. 67(2), pp. 263–277 (2018)

DOI 10.24425/119639

# The DC-side active filter with dual-buck full-bridge inverter for wind generators

XIAO-QIANG CHEN[1,2], SHOU-WANG ZHAO[1], YING WANG[1]

[1] *School of Automation and Electrical Engineering*
*Lanzhou Jiaotong University*
*Anning West Road 88, Anning District, Lanzhou, 730070, China*
*email: xqchen@mail.lzjtu.cn*

[2] *Key Laboratory of Opto-Electronic Technology and Intelligent Control*
*Ministry of Education, Lanzhou Jiaotong University*
*Anning West Road No. 88, Anning District, Lanzhou, 730070, China*

(Received: 07.05.2017, revised: 28.12.2017)

**Abstract:** This paper proposes a new dc-side active filter for wind generators that combines 12-pulse polygon auto-transformer rectifier with dc-side current injection method and dual-buck full-bridge inverter having not the "shoot-through" problem in conventional bridge-type inverters, and therefore this system with the character low harmonic distortion and high reliability. The proposed dc-side active filter is realized by using dual-buck full bridge converter, which directly injects compensation current at dc-side of two six-pulse diode bridges rectifiers. Compared with the conventional three-phase active power filter at ac-side, the system with the dc-side active filter draws nearly sinusoidal current by shaping the diode bridges output current to be triangular without using the instantaneous reactive power compensation technology, only using simple hysteretic current control, even though under load variation and unbalanced voltage disturbances, and while an acceptable linear approximation to the accurate waveform of injection current is recommended. The performance of the system was simulated using MATLAB/Simulink, and the possibility of the dc-side active filter eliminating current harmonics was confirmed in steady and transient states. The simulation results indicate, the system has a total harmonic distortion of current reduced closely to 1%, and a high power factor on the wind generator side.

**Key words:** multi-pulse ac-dc converter, auto-transformer, harmonic suppression, DC-side active filter, dual-buck full-bridge inverter

## 1. Introduction

With the global energy crisis and environmental problems increasingly prominent, the demand for renewable energy source is growing drastically. Wind power, an emerging, free, inexhaustible clean energy source, is received increasingly more attention, which can be relied

on for the long-term future [1]. In recent years, the permanent-magnet synchronous generators (PMSGs) meet increasing application in wind turbines industry owing to the development of the permanent-magnet materials [2]. However, the soaring growth in capacity of wind turbines brings new problems and challenges, especially focus on the generator rectification side [3–5]. The generator side converter of PMSGs can be a passive (diode bridge) rectifier, an active (pulse width modulated, PWM) rectifier or a hybrid rectifier. Diode-bridges rectifiers are less expensive and inherently higher reliable than PWM converters [4, 5]. However, the large number of harmonics in PMSG stator current are harmful to wind turbines generators, which will greatly increase current ripple and torque pulsation, and then increase the copper and iron losses, and reduce the generator efficiency. Therefore, in order to solve harmonic pollution problem of WECSs, various passive, active, or hybrid filters are used in rectification side of PMSGs, but passive filters are bulky, while active filters require complex control. And the power rating of these filters may be close to the ratings of the load, leading to increased losses, cost, and control complexity, especially in high power wind generation occasion [6–8].

Multi-pulse rectification technique with phase shifted transformers are proposed to reduce stator current ripples and torque pulsation [5–11]. Multipulse AC-DC converter has advantages of high reliability, simple control, and low cost for harmonic mitigation, which is very suitable for medium and high power applications. However, with increased pulse number, especially using the 18, 24, 36-pulse or more multi-pulse rectifiers in order to meet the international power quality standards, such as IEEE 519-1992 (IEEE 1992) and IEC 61000-3-2 (IEC 2014), the cost, component count and complexity of the phase shifting transformer is increased, which make it restricted for WECSs. The 12-pulse rectifier is a good trade-off between harmonic reduction and system complexity, and is commonly used in the industry. However, the 12-pulse AC-DC converter alone does not efficiently reduce the ac-side harmonics to the relevant standards' levels.

This paper proposes a low harmonic 12-pulse polygon auto-transformer AC-DC converter with current directly-injection at dc-side, in order to eliminate ac-side harmonics of 12-pulse rectifiers efficiently and effectively and achieve better power quality. This paper is organized as follows: Firstly, the paper gives the description about the polygon auto-transformer. Secondly, the detailed theoretical analysis of the dc-side current directly-injection method is taken into account. The method looking like dc side active filter, is realized by using an additional dual-buck full-bridge inverter having not shoot through state, which directly injects compensation current at DC side of the two six-pulse diode bridges rectifiers. Thirdly and the last, gives a simulation results and discussion using MTLAB/Simulink in order to better evaluation and to show the correctness of the theoretical analysis and feasibility of the proposed power converter and its control strategy.

## 2. Description of system

Fig. 1 shows architecture and the general configuration of the proposed 12-pulse rectifier with the DC side active power filter (DC-APF), which consists of PMSG, a polygon auto-transformer (PAT), two three-phase diode bridges, an interphase transformer (IPT), and the dual-buck full-bridge inverter (DBFI) and load (including DC/DC and grid-connected inverter).

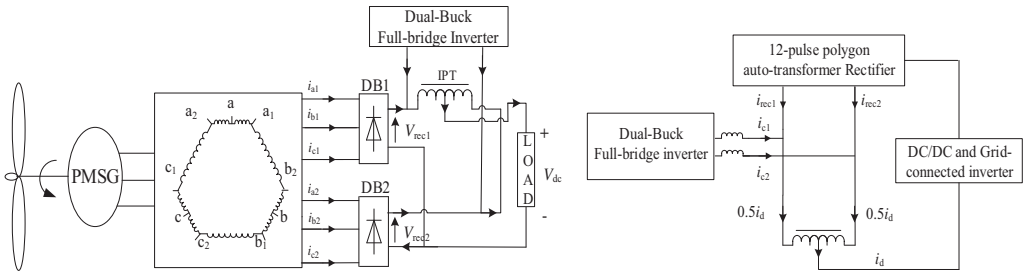


Fig. 1. Architecture of the proposed 12-pulse rectifier with dc-side active filter (see (a)) and the general configuration of 12-pulse rectifier with dc side active power filter (see (b))

Fig. 2 shows the magnetic circuit, the phasor diagram and the coupling circuit of the PAT. The two sets of three-phase voltages with 30° phase-shift from each other are connected to the two diode rectifiers. The output of the DBFI directly connect to two diode bridges output top terminals and compensation currents flow two non-common terminals of IPT.

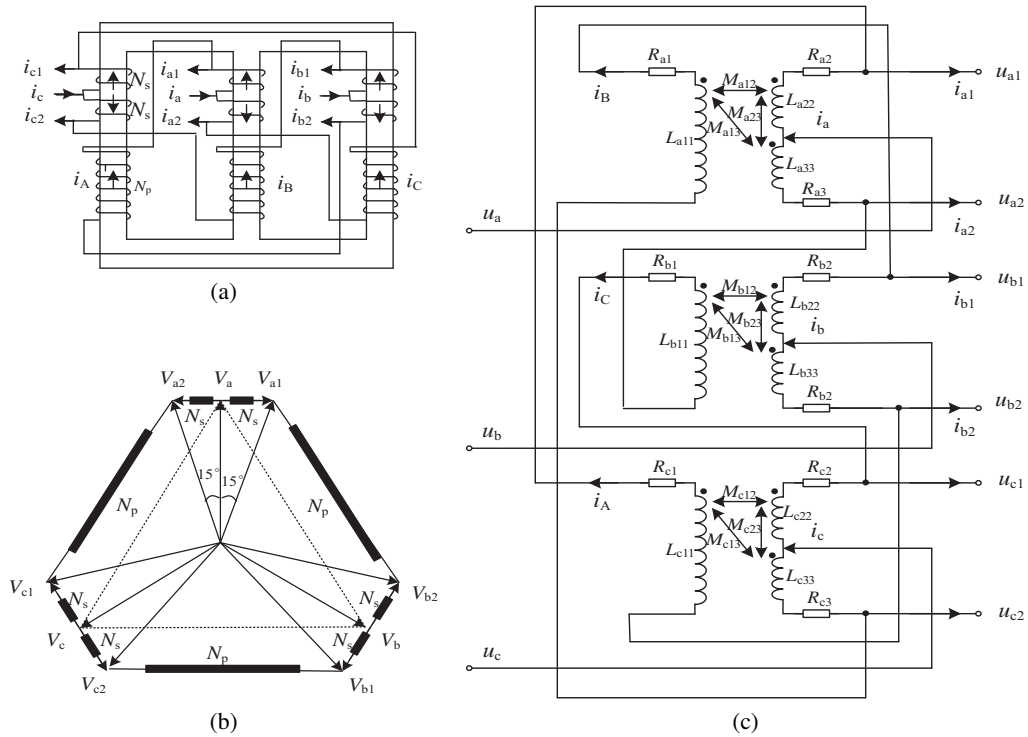


Fig. 2. The magnetic circuit, the phasor diagram and the coupling circuit of the polygon auto-transformer: (a) the magnetic circuit; (b) the phasor diagram; (c) the coupling circuit

For the PAT without the DC-APF, in Fig. 2, $N_p$ and $N_s$ are the turn number of the PAT long windings and short windings respectively, and in order to achieve 30° phase shift between the two sets of three phase voltage ($V_{a1}$, $V_{b1}$, $V_{c1}$) and ($V_{a2}$, $V_{b2}$, $V_{c2}$), they should fulfill:

$$N_p : N_s = 2\left(\sqrt{3}-1\right) : \left(2-\sqrt{3}\right). \tag{1}$$

According to magnetomotive forces (MMF) balance and Kirchhoff's Current Law (KCL), the relationship between the input current ($i_a$, $i_b$, $i_c$) and the output current ($i_{a1}$, $i_{b1}$, $i_{c1}$) and ($i_{a2}$, $i_{b2}$, $i_{c2}$) of the polygon autotransformer can be obtained as follows:

$$\begin{cases} i_a = i_{a1} + i_{a2} + \dfrac{N_s(i_{b2} - i_{b1} + i_{c1} - i_{c2})}{N_s + N_p} \\ i_b = i_{b1} + i_{b2} + \dfrac{N_s(i_{c2} - i_{c1} + i_{a1} - i_{a2})}{N_s + N_p} \\ i_c = i_{c1} + i_{c2} + \dfrac{N_s(i_{a1} - i_{a1} + i_{b1} - i_{b2})}{N_s + N_p} \end{cases}. \tag{2}$$

The Fourier series expression of input current of phase a can be expressed as:

$$i_a = \frac{2I_d}{\pi} \sum_{n=1,11,13\cdots}^{\infty} \frac{1}{n}\left[1 + \frac{N_s}{N_s+N_p}\cos\frac{n\pi}{12} + \frac{N_s}{N_s+N_p}\cos\frac{3n\pi}{12} + \right.$$
$$\left. + \frac{2N_s}{N_s+N_p}\cos\frac{5n\pi}{12}\cdots\right]\sin(n\omega t). \tag{3}$$

From the expression (3), the input currents of the PAT contains harmonic components of $12k \pm 1$ ($k$: integer). The total harmonic distortion (THD) without current injection at dc-side is about 15.22%. Therefore, the 12-pulse AC-DC converter alone and without the DC-APF does not efficiently reduce the ac-side harmonics to the relevant standards' levels IEEE 519-1992 and IEC 61000-3-2.

### 2.1. The required harmonic current analysis

By analyzing the operation of 12-pulse rectifier, the ac-side current draw near sinusoidal currents by shaping the two diode rectifier output currents to be triangular, while diode rectifier input currents are also to become triangular, compared to quasi-square waveform without any harmonic suppression compensation methods. Fig. 3 shows the required construction of current when the ac-side current of 12-pulse rectifier draw near sinusoidal currents. Fig. 3(a) is the rectifier input current waveforms of 12-pulse rectifier under draw near sinusoidal currents. Fig. 3(b) is the dc-side waveforms of two six-pulse rectifiers under draw near sinusoidal currents.

In order to simplify the analysis, the switching function $S$ (shown in Fig. 3(b)) is introduced, which could make input current straight-forward and easy expressed by the injection current of dual-buck inverter and output current of the two six-pulse rectifier. The switching function with commutation effect is equal to 1 or $-1$ in the non-overlap conducting period, to 0.5 or $-0.5$ in the overlap period, and to zero in the interrupted period. [$S_{a1}$ $S_{b1}$ $S_{c1}$] is the switching function

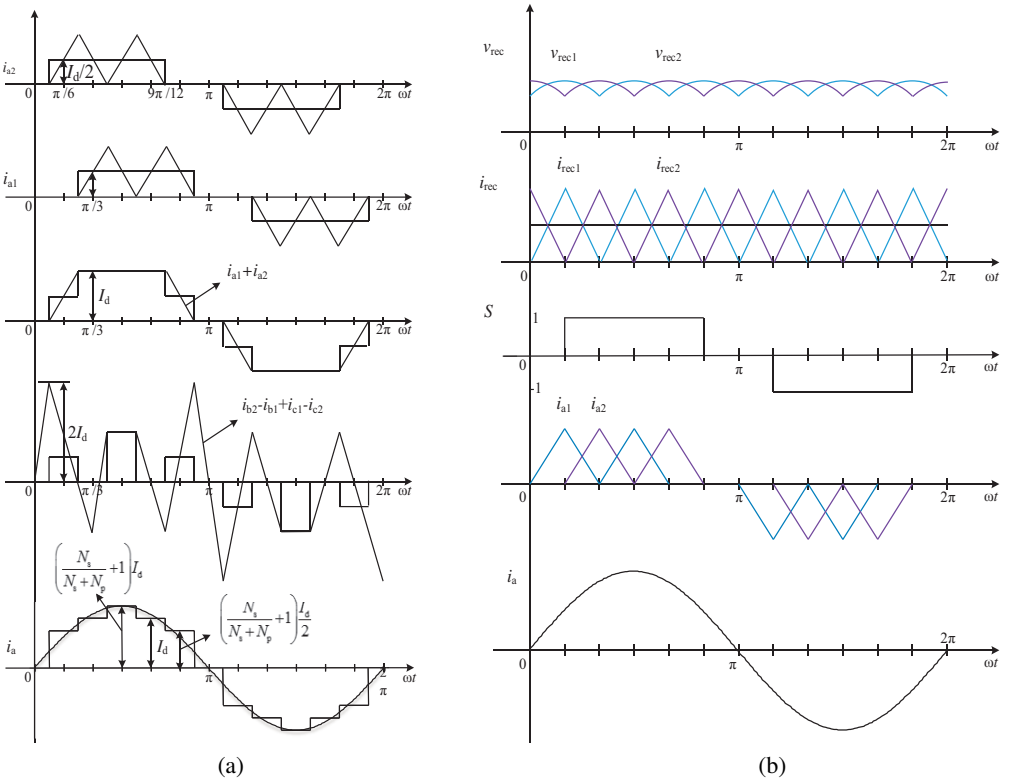


(a) (b)

Fig. 3. The required current construction of 12-pulse rectifier with DC side current injection: (a) the rectifier input current waveforms of 12-pulse rectifier under draw near sinusoidal currents; (b) DC side waveforms of 12-pulse rectifier under draw near sinusoidal currents

phase a1, b1 and c1 respectively. Therefore, the output currents of the PAT can be expressed by switching functions and the output currents of the six-pulse bridges as follows:

$$\begin{bmatrix} i_{a1} \\ i_{b1} \\ i_{c1} \end{bmatrix} = \begin{bmatrix} S_{a1} \\ S_{b1} \\ S_{c1} \end{bmatrix} i_{rec1}, \quad \begin{bmatrix} i_{a2} \\ i_{b2} \\ i_{c2} \end{bmatrix} = \begin{bmatrix} S_{a2} \\ S_{b2} \\ S_{c2} \end{bmatrix} i_{rec2}, \quad \begin{cases} S_{a2} = S_{a1}\angle 30^\circ \\ S_{b2} = S_{b1}\angle 30^\circ \\ S_{c2} = S_{c1}\angle 30^\circ \end{cases}, \tag{4}$$

where $i_{rec1}$ and $i_{rec2}$ are the dc-side currents of the two diode bridges, respectively, $S_{a1}$, $S_{a2}$, $S_{b1}$, $S_{b2}$, $S_{c1}$ and $S_{c2}$ are the switching functions of phases a1, a2, b1, b2, c1 and c2, respectively. Here, the switching function $S_{a1}$ for phase a1 is given by:

$$S_{a1} = \frac{2\sqrt{3}}{\pi}\left(\sin(\omega t) - \frac{1}{5}\sin(5\omega t) - \frac{1}{7}\sin(7\omega t) + \frac{1}{11}\sin(11\omega t) + \frac{1}{13}\sin(13\omega t)\cdots\right). \tag{5}$$

Then, according to KCL and MMF balance, we can get the relationship among output currents [$i_{rec1}$, $i_{rec2}$] of the two six-pulse rectifiers, the injecting compensation current $i_{c1}$ and $i_{c2}$ of

the DC-APF, and the load current $i_d$ as follows:

$$\begin{bmatrix} i_{rec1} \\ i_{rec2} \end{bmatrix} = \begin{bmatrix} \frac{I_d}{2} - i_{c1} \\ \frac{I_d}{2} - i_{c2} \end{bmatrix}. \tag{6}$$

The practical compensation currents, according to principles of electric circuits, one flow out of the compensation main circuit, and another flow into the main circuit, operate in the complementary state and mode, therefore the injecting compensation current can be expressed as $i_x = i_{c1} = -i_{c2}$. Assuming that the input current of the three-phase source are the sinusoidal since the injecting compensation current. Substituting (4) and (6) into (2), the phase currents of the three-phase source are expressed as:

$$\begin{cases} i_a = 0.5A_1 I_d + A_2 i_x \\ i_b = 0.5B_1 I_d + B_2 i_x \\ i_c = 0.5C_1 I_d + C_2 i_x \end{cases}. \tag{7}$$

where,

$$\begin{cases} A_1 = S_{a1} + S_{a2} + \dfrac{N_s}{N_s + N_p}(S_{b2} - S_{b1} + S_{c1} - S_{c2}) \\ A_2 = S_{a1} - S_{a2} + \dfrac{N_s}{N_s + N_p}(-S_{b2} - S_{b1} + S_{c1} + S_{c2}) \\ B_1 = S_{b1} + S_{b2} + \dfrac{N_s}{N_s + N_p}(S_{c2} - S_{c1} + S_{a1} - S_{a2}) \\ B_2 = S_{b1} - S_{b2} + \dfrac{N_s}{N_s + N_p}(-S_{c2} - S_{c1} + S_{a1} + S_{a2}) \\ C_1 = S_{c1} + S_{c2} + \dfrac{N_s}{N_s + N_p}(S_{a2} - S_{a1} + S_{b1} - S_{b2}) \\ C_2 = S_{c1} - S_{c2} + \dfrac{N_s}{N_s + N_p}(-S_{a2} - S_{a1} + S_{b1} + S_{b1}) \end{cases}.$$

Because of three-phase input current ($i_a$, $i_b$, $i_c$) are sinusoidal, the injecting compensation current $i_x$ of full-bridge inverter can be solved:

$$i_x = \frac{0.5I_d \left[ B_1 \sin(\omega t) - A_1 \sin\left(\omega t - \frac{2\pi}{3}\right) \right]}{A_2 \sin\left(\omega t - \frac{2\pi}{3}\right) - B_2 \sin(\omega t)}. \tag{8}$$

However, since each part of Equations (8) are expressed by Fourier series, it is difficult to calculate the exact injection currents directly in practical circuit. Therefore, an acceptable linear approximation to the accurate and theoretical waveform of injection current are calculated by MATLAB, as shown in Fig. 4. It can be concluded that the wave-shape of the injecting compensation current is exactly like a six-time frequency triangular wave. Therefore, in order to facilitate the analysis and implementation, there is speculation that, by directly injecting an approximated triangular compensation current by the dual-buck full-bridge inverter, a near sinusoidal input current also could be obtained.

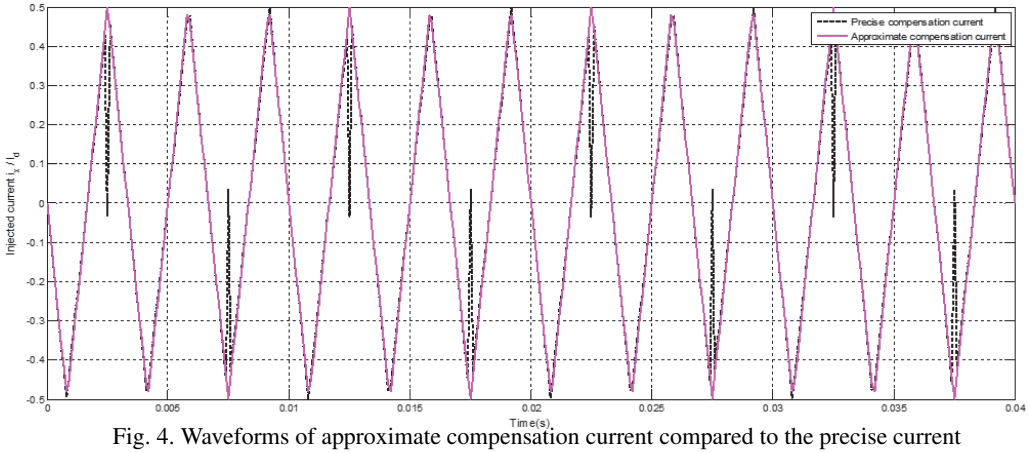


Fig. 4. Waveforms of approximate compensation current compared to the precise current

### 2.2. DC-side active power filter

Fig. 5 show the circuit construction and control block diagram of the proposed dc-side active power filter with the dual-buck full-bridge converter. The control block is design in order to product the gating signal generator for the DBFI. The reference for the injection current is synchronized with the output voltage of the auto-transformer, which product the six-time frequency synchronous triangular current waveform by circuits of the standard digital logic and phase locked loop electronic devices. The averaged dc-side output current are detected and fed to the DC-APF, then the DC-APF controller calculate the reference compensation current. The

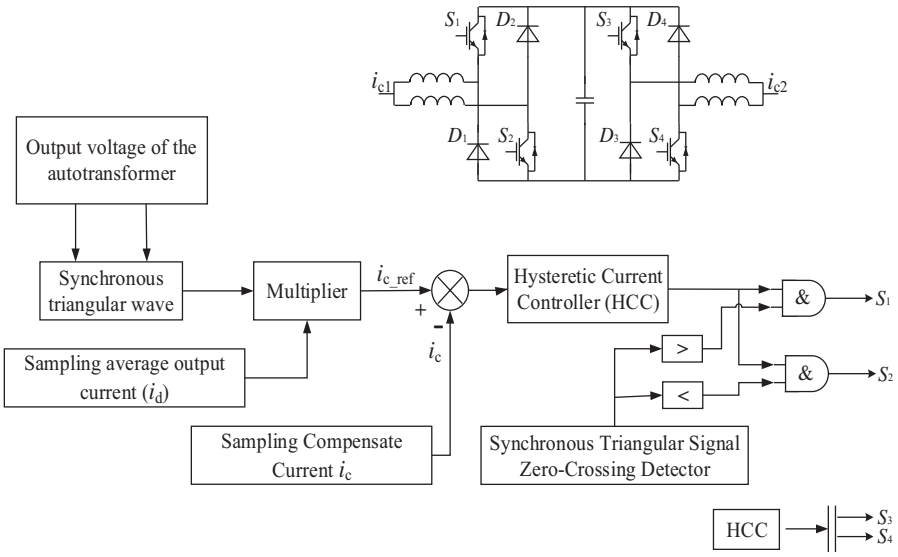


Fig. 5. The system diagram and control block diagram of the dc-side active power filter

reference current $i^*_{c\_ref}$ is generated by multiplying the averaged dc-side output current and the produced the synchronous triangular signal. The reference injection current and the practical feedback compensation currents $i_c$ will send into the current controller, and then the current error that produced by using a hysteretic current controler (HCC), finally gating signals generated and obtained by logic circuits between the HCC current error and synchronous triangular signal zero-crossing detector for DBFI. Compared with the conventional three-phase active power filter at ac-side, the system with the dc-side active filter draws nearly sinusoidal current by shaping the diode bridges output current to be triangular without using the instantaneous reactive power compensation technology, only using simple hysteretic current control and some simple logic circuits.

Fig. 6 is the four switching states for dual-buck converter under the six-times of line frequency (300 Hz, for 50 Hz grid) synchronous triangular signal. The compensation performance usually is deteriorated by the limited switching frequency and dead time that needs and requires smaller frequency and lager dead-time, considering the requirement of high reliability. The phase-leg of the traditional converter based DC/AC or AC/DC converter, bridge-type converter, and active power filter is composed of two power switches that a dead-time is required in order to avoid the "shoot-through" phenomenon, while the dual-buck bridge converter composed of one power switch and one diode without dead-time due to the phase-leg composed by $S_1$ and $D_1$ (or $S_3$ and $D_3$) operates in the synchronous triangular signal positive half cycle, and the other $S_2$ and $D_2$ (or $S_4$ and $D_4$) in the negative half cycle. Therefore, the switching frequency of the dc-side active power filter could be increased for further. Here, the dual-buck inverter topology is specially proposed for APF applications [9] where high reliability is required, the hysteresis band width is 2A, the switching frequency of the dual buck inverter is 12 kHz.

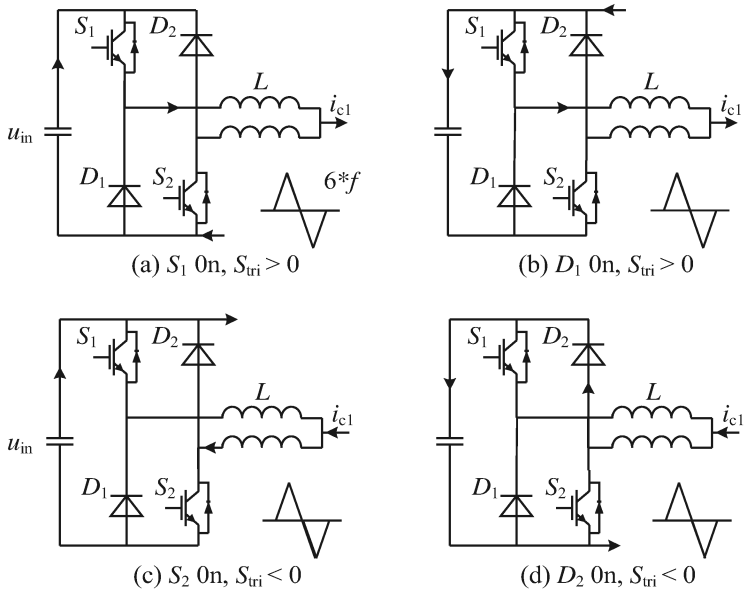


Fig. 6. The four switching operation states and equivalent circuit for dual-buck converter under the six-times of line frequency (300 Hz, for 50 Hz grid) synchronous triangular signal

# 3. Simulation and simulation results

## 3.1. Simulation

The Sim-Power-Systems Toolbox in Simulink is used to model and simulate the proposed WECS system, in order to verify the correctness of theoretical analysis. The main parameters of the proposed WECS system are given in Table 1.

Table 1. Parameters of the proposed WECS

| Parameter | Rated power | Winding resistance $R$/ Winding inductance $L$ | Interphase transformer | Hysteresis band width | Switching frequency of the DC-APF | Output inductances of the DC-APF | DC side capacitors of the DC-APF |
|---|---|---|---|---|---|---|---|
| Value | 10 kW | $R$=1.73 Ω / $L$=6.5 mF | 10 mH | 2 A | 12 kHz | 400 $\mu$H | 1 mF |
| Transformer long windings $N_p$ : short windings $N_s$ | | | | 284 : 52 | Standard/reference | IEEE 519-1992 / IEC 61000-3-2 | |

## 3.2. Simulation results

When the dual-buck full bridge inverter inject compensation current $i_x$ in $t = 0.2$ s, the corresponding simulation results of overall AC-side PMSG stator current waveforms and its harmonic spectrum are shown in Fig. 7. Fig. 7(a) is three-phase PMSG stator current waveforms during the active moment of the compensation; Fig. 7(b) is the harmonic spectrum of AC mains current without using dc-side current injection method. The THD of polygon auto-transformer based 12-pulse rectifier without DC side current injection is 12.05%, which contains a large amount of $11^{th}$ and $13^{th}$ harmonic components; Fig. 7(c) is the harmonic spectrum of AC mains current with using dc-side current injection method. The THD of polygon auto-transformer based 12-pulse rectifier with DC side active power filter is 1.48%, which can be seen that the power quality is improved greatly. The comparison data results of the PMSG stator currents power quality with and without injection currents are given in Table 2. Table 3 shows the comparison

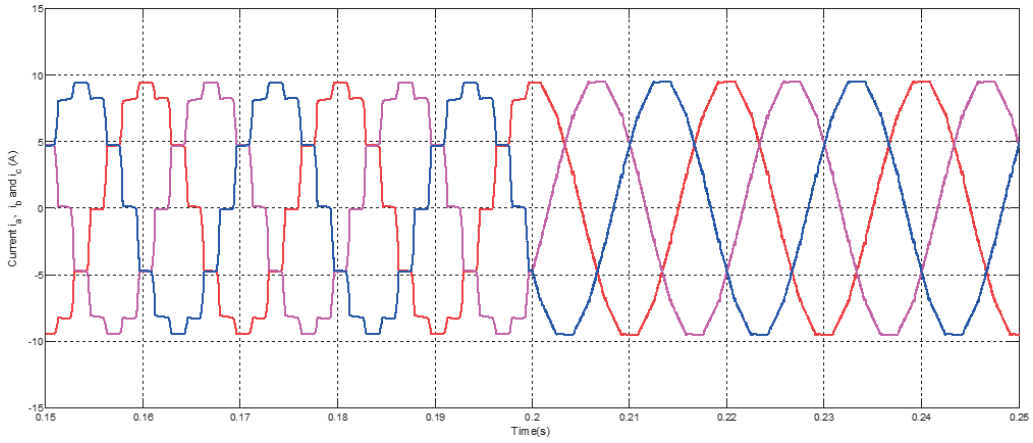


Fig. 7(a) Overall ac-side PMSG stator current waveforms during the active moment of the compensation

results of various power quality indices. Furthermore, the proposed system can still better work as a normal and standard 12-pulse auto-transformer rectifier, compared to conventional passive diode bridge rectifier, even if the DC-APF is non-connected or control-malfunctioned.

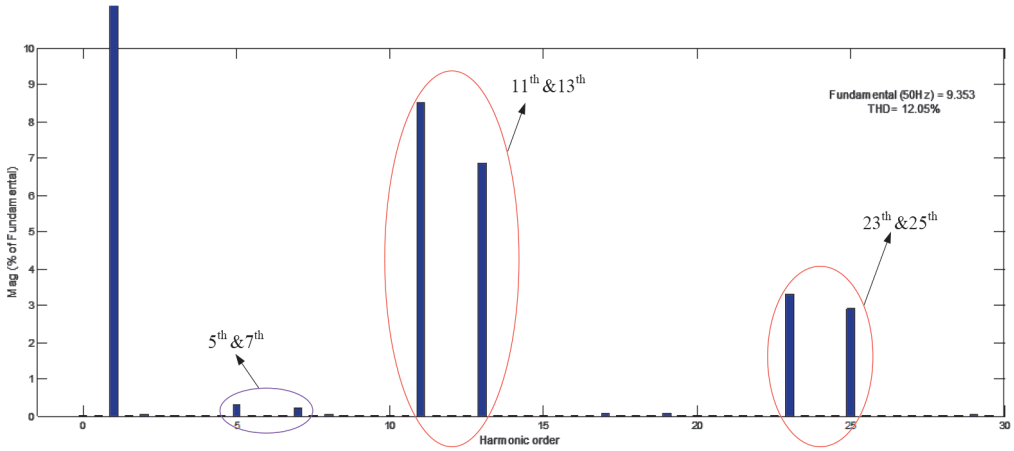


(b) Harmonic spectrum of AC mains current without using dc-side current injection method

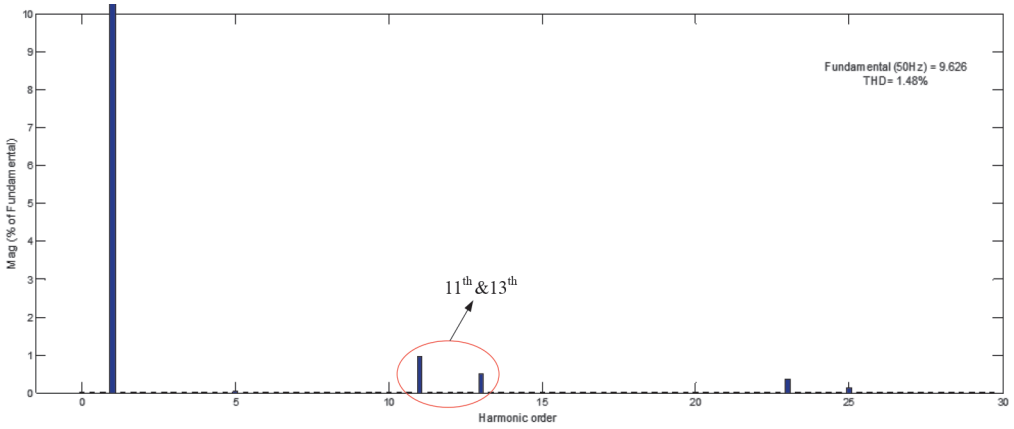


(c) Harmonic spectrum of AC mains current with using dc-side current injection method

Fig. 7. Overall AC-side PMSG stator current waveforms and its harmonic spectrum

Table 2. Comparison of the THD of input line current with and without injection current

| Injection current | Input current | $THD_i$ | Fundamental (rms value) | $5^{th}$ harmonics | $7^{th}$ harmonics | $11^{th}$ harmonics | $13^{th}$ harmonics |
|---|---|---|---|---|---|---|---|
| **without** | $i_a$ | 12.05% | 6.613 A | 0.30% | 0.21% | 8.53% | 6.88% |
| **with** | $i_a$ | 1.48% | 6.806 A | 0.02% | 0.02% | 0.96% | 0.48% |

Table 3. Comparison of various power quality indices with and without injection current

| **Injection current** | ***THD*$_i$ (%)** | **$I_s$ (A)** | **$V_d$ (V)** | ***PF*** | ***DPF*** | ***DF*** |
|---|---|---|---|---|---|---|
| **without** | 12.05 | 6.66 | 229.03 | 0.998 | 0.996 | 0.993 |
| **with** | 1.48 | 6.81 | 230.34 | 0.999 | 0.999 | 0.999 |

Notes: $THD_v$ – the THD of PMSG stator voltage; $THD_i$ – the THD of PMSG stator current; $I_s$ – the rms value of PMSG stator current; $V_d$ – the average value of rectifier output voltage; *PF* – the power factor; *DPF* – the displacement power factor; *DF*: the distortion factor.

The injection current and output current waveforms of one of the two six-pulse diode bridges are given in Fig. 8. Waveforms of the dc-side injection current and the output current of diode

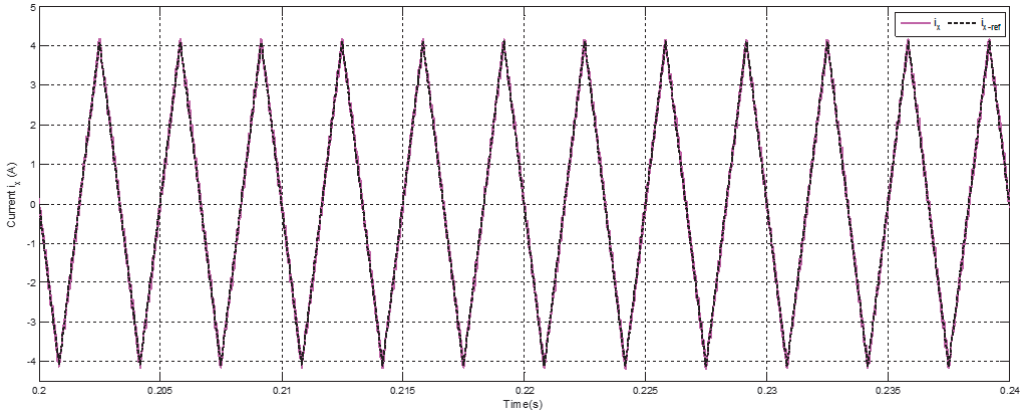


(a) The dc-side injection current

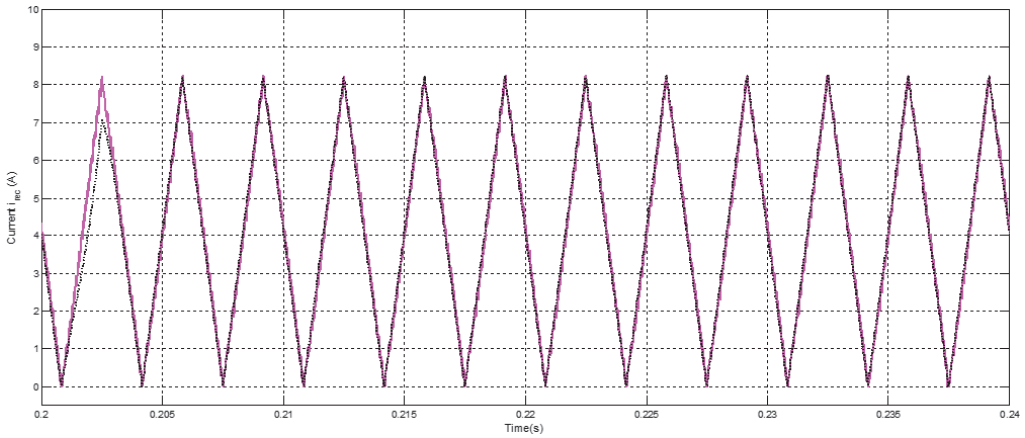


(b) The output current of diode bridge when using dc-side current injection

Fig. 8. The injection current and output current of six-pulse diode bridge

bridge after injecting compensation current are triangular-shape waveforms. The output currents $i_{a1}$ and $i_{a2}$ of auto-transformer are given in Fig. 9(a). It has to be noted that the currents $i_{a1}$ and $i_{a2}$ will change from quasi-square waveforms to triangular waveforms after injecting the compensation current, which also shows the 30° phase shifts provided by the PAT. Fig. 9(b) is the rectifier output voltage waveforms. Rectifier output voltage is somewhat higher than that of 12-pulse rectifier without DC-APF. Fig. 10 is the simulation results in phase-a under various load perturbation including various inductive loads (Full load parameter: 9.5 mH/28 Ω) and capacitive loads (Full load parameter: 100 $\mu$F/28 Ω). The simulation results show the THD of the stator current in phase-a and power factor without and with DC-APF's compensation, which could be observed that the system with DC-APF can perfectly meet and fulfill the IEEE standard 519-1992 (THD $<$ 5%) under various load conditions, while obtain effectively higher power factor close to 100%.

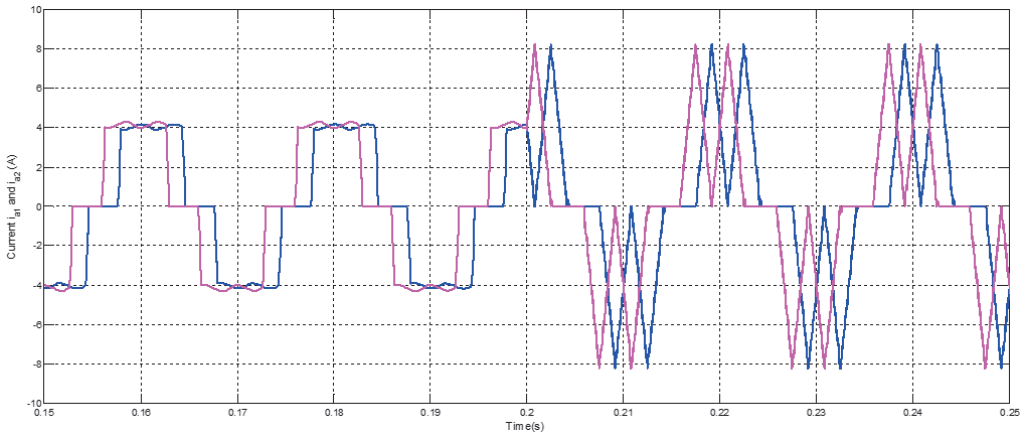


(a) The output current waveforms of auto-transformer

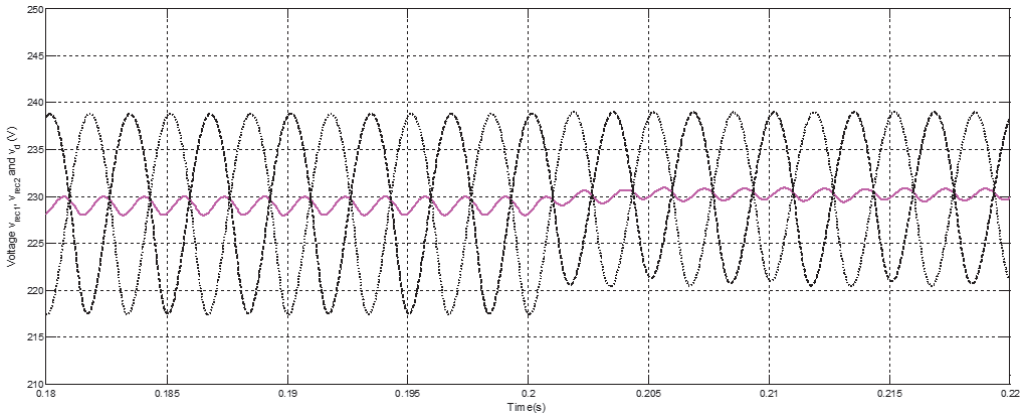


(b) The rectifier output voltage waveforms

Fig. 9. The output current of auto-transformer and rectifier output voltage waveforms during using dc-side current injection

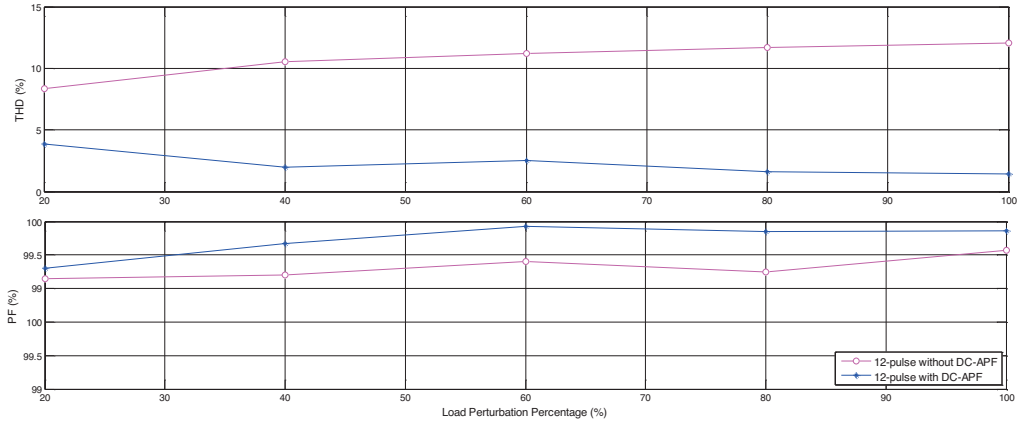


(a) Under inductive load (full load parameter: 9.5 mH/28 Ω)

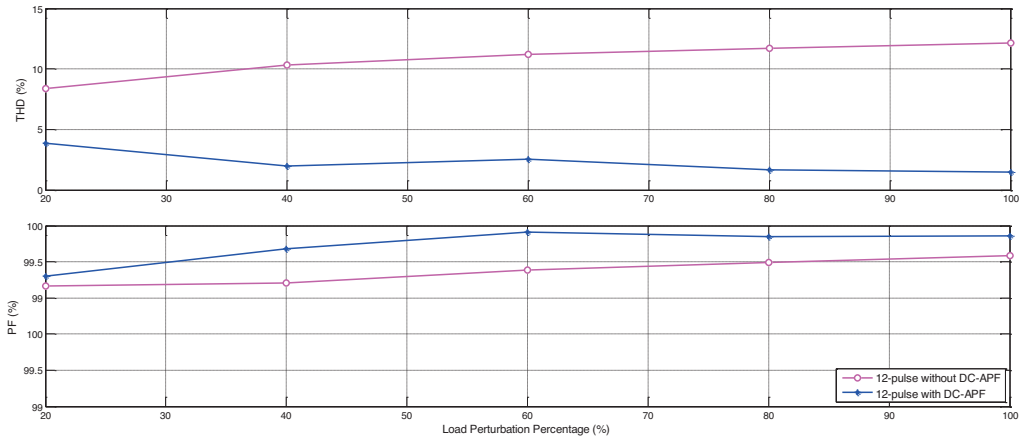


(b) Under capacitive load (full load parameter: 100 $\mu$F/28 Ω)

Fig. 10. Simulation results in phase-a under various load perturbation

The performance affected by unbalanced auto-transformer is investigated. Table 4 is the comparison of the THD of input line current with and without injection current under unbalance auto-transformer by changing the polygon long windings and short windings from the three turn number 284 : 52 : 52, 284 : 52 : 52, 284 : 52 : 52 to 284 : 38 : 52, 284 : 38 : 38, 210 : 38 : 38. It is obviously that the ac-line currents and the output current waveforms of auto-transformer are unbalanced with different amplitudes and harmonic currents before the active DC-APF due to the unbalanced auto-transformer. After injecting the compensation currents, the performance of the system is investigated, which demonstrate that the DC-APF inproves the linecurrent quality and mitigates the main effects caused by unbalanced auto-transformer. The proposed system also demonstrate fast dynamic response for compensating the current harmonic and compensation performance.

Table 4. Comparison of input current with and without injection current under unbalance transformer

| Injection current | Input current | $THD_i$ | Fundamental (rms value) | $5^{th}$ harmonics | $7^{th}$ harmonics | $11^{th}$ harmonics | $13^{th}$ harmonics | $17^{th}$ harmonics |
|---|---|---|---|---|---|---|---|---|
| **without** | $i_a$ | 12.57% | 6.520 A | 3.89% | 2.12% | 7.82% | 6.25% | 2.39% |
| | $i_b$ | 12.31% | 6.677 A | 3.55% | 3.31% | 7.07% | 6.66% | 2.46% |
| | $i_c$ | 12.79% | 6.343 A | 3.10% | 1.71% | 8.91% | 6.21% | 2.08% |
| **with** | $i_a$ | 3.14% | 6.721 A | 2.25% | 1.10% | 1.25% | 0.33% | 0.44% |
| | $i_b$ | 2.60% | 6.830 A | 1.39% | 0.90% | 1.26% | 0.35% | 0.40% |
| | $i_c$ | 3.93% | 6.566 A | 2.96% | 1.68% | 1.06% | 0.29% | 0.40% |

## 4. Conclusion

In this paper, a low harmonic 12-pulse polygon auto-transformer rectifier with dc-side active power filter using directly current injection method for wind generation system is proposed. The compensation strategy is investigated and an acceptable linear approximation to the accurate waveform of injection current is recommended, which can effectively improve power quality. The THD of stator current is about l.48%, and various power quality indices are improved greatly, which can meet the various international power quality standards. Moreover, the dual-buck full-bridge inverter is an alternative power conversion topology that has better efficiently and higher performances due to eliminating "shoot-through" phenomenon. Simulation results show the correctness of the theoretical analysis and feasibility of the proposed power converter and its control strategy.

**Acknowledgements**

The authors wish to thank the project supported by the Natural Science Foundation of Gansu Province Education Department (2017A-020), the National Natural Science Foundation of China (51767013), the Science and Technology Research and Development Plan of China Railway Corporation (2017J012-A).

**References**

[1] Yaramasu V., Dekka A., Durán M.J. *et al.*, *PMSG-based Wind Energy Conversion Systems: Survey on Power Converters and Controls*, IET Electric Power Applications, vol. 11, no. 6, pp. 956–968 (2017).

[2] Hossain M.M., Ali M.H., *Future Research Directions for the Wind Turbine Generator System*, Renewable and Sustainable Energy Reviews, vol. 49, pp. 481–489 (2015).

[3] Tripathi S.M. *et al.*, *Grid-integrated Permanent Magnet Synchronous Generator based Wind Energy Conversion Systems: A technology review*, Renewable and Sustainable Energy Reviews, vol. 51, pp. 1288–1305 (2015).

[4] De Freitas T.R.S. *et al.*, *Rectifier Topologies for Permanent Magnet Synchronous Generator on Wind Energy Conversion Systems: A Review*, Renewable and Sustainable Energy Reviews, vol. 54, pp. 1334–1344 (2016).

[5] Damin Z., Shitao W. *et al.*, *Predictive Fast DSP-Based Current Controller for a 12-pulse Hybrid-Mode Thyristor Rectifier*, IEEE Transactions on Power Electronics, vol. 28, no. 11, pp. 5263–5271 (2013).

[6] Xia C., Wang Z. *et al.*, *A Novel Cascaded Boost Chopper for the Wind Energy Conversion System based on the Permanent Magnet Synchronous Generator*, IEEE Transactions on Energy Conversion, vol. 28, no. 3, pp. 512–522 (2013).

[7] Singh B., Gairola S., Singh B.N. *et al.*, *Multipulse AC–DC Converters for Improving Power Quality: A Review*, IEEE Transactions on Power Electronics, vol. 23, no. 1, pp. 260–281 (2008).

[8] Young C.M., Wu S.F. *et al.*, *A DC-Side Current Injection Method for Improving AC Line Condition Applied in the 18-pulse Converter System*, IEEE Transactions on Power Electronics, vol. 29, no. 1, pp. 99–109 (2014).

[9] Chen J. *et al.*, *Harmonics Attenuation and Power Factor Correction of a More Electric Aircraft Power Grid Using Active Power Filter*, IEEE Transactions on Industrial Electronics, vol. 63, no. 12, pp. 7310–7319 (2016).

[10] Yao Z., Xiao L., Yan Y., *Dual-Buck Full-Bridge Inverter with Hysteresis Current Control*, IEEE Transactions on Industrial Electronics, vol. 56, no. 8, pp. 3153–3160 (2009).

[11] Khan A.A., Cha H., *Dual-Buck-Structured High-Reliability and High-Efficiency Single-Stage Buck–Boost Inverters*, IEEE Transactions on Industrial Electronics, vol. 65, no. 4, pp. 3176–3187 (2018).